



HAL
open science

Peculiar tension wood structure in *Laetia procera* (Poepp.) Eichl. (Flacourtiaceae)

Julien Ruelle, Masato Yoshida, Bruno Clair, Bernard Thibaut

► **To cite this version:**

Julien Ruelle, Masato Yoshida, Bruno Clair, Bernard Thibaut. Peculiar tension wood structure in *Laetia procera* (Poepp.) Eichl. (Flacourtiaceae). *Trees - Structure and Function*, 2007, 21 (3), pp.345-355. 10.1007/s00468-007-0128-0 . hal-00194923

HAL Id: hal-00194923

<https://hal.science/hal-00194923>

Submitted on 7 Dec 2007

HAL is a multi-disciplinary open access archive for the deposit and dissemination of scientific research documents, whether they are published or not. The documents may come from teaching and research institutions in France or abroad, or from public or private research centers.

L'archive ouverte pluridisciplinaire **HAL**, est destinée au dépôt et à la diffusion de documents scientifiques de niveau recherche, publiés ou non, émanant des établissements d'enseignement et de recherche français ou étrangers, des laboratoires publics ou privés.

Julien Ruelle • Masato Yoshida • Bruno Clair • Bernard Thibaut

Peculiar tension wood structure in *Laetia procera* (Poepp.) Eichl.
(Flacourtiaceae)

J. Ruelle (Contact), B. Thibaut

UMR EcoFoG, Campus agronomique - BP 709, 97387 Kourou cedex, Guyane Française

Tel. +594594320347; Fax +594594323281

e-mail: ruelle_j@kourou.cirad.fr

M. Yoshida

School of Bioagricultural Sciences, Nagoya University, Chikusa,

Nagoya 464-8601, Japan

B. Clair

Laboratoire de Mécanique et Génie Civil (LMGC)

UMR 5508, CNRS - Université Montpellier 2

Place E. Bataillon, cc 048, 34095 Montpellier Cedex 5, France

1 ABSTRACT

2 Tension wood of *Laetia procera* (Poepp.) Eichl. (Flacourtiaceae), a neo-tropical forest
3 species, shows a peculiar secondary wall structure, with an alternance of thick and thin
4 layers, while opposite wood of this species has a typical secondary wall structure
5 (S1+S2+S3). Samples for the study of microstructural properties were collected upon
6 estimation of growth stresses in the living tree, in order to analyse correlation of the
7 former with the latter. Investigation using optical microscopy, scanning electron
8 microscopy and UV microspectrophotometry allowed the description of the anatomy,
9 ultra-structure and chemistry of this peculiar polylaminate secondary wall. In the thick
10 layers, cellulose microfibril angle is very low (i.e., microfibril orientation is close to fibre
11 axis) and cellulose microfibrils are well organised and parallel to each other. In the thin
12 layers, microfibrils (only observable in the inner layer) are less organised and are oriented
13 with a large angle relative to the axis of the cell. Thick layers are lightly lignified
14 although thin layers show a higher content of lignin, close to that of opposite wood
15 secondary wall. The more the wood was under tensile stress, the less the secondary wall
16 was lignified, and the lower the syringyl on guaiacyl lignin units ratio was. The innermost
17 layer of the secondary wall looks like a typical S3 layer with large microfibril angle and
18 lignin occurrence. The interest of this kind of structure for the understanding of stress
19 generation is discussed.

20

21 **Keywords** Tension wood · Tropical rainforest species · UV microspectrophotometry ·
22 Scanning Electron Microscopy · Cellulose microfibril angle

23 INTRODUCTION

24 In order to restore their verticality after accidental leaning, to maintain the branch at a
25 given angle or to change axis orientation to reach the canopy for better access to light
26 trees are able to bend progressively their trunk or branches by a very active mechanical
27 action driven by cambial activity (Sinnott 1952). This reorientation is associated with the
28 formation of a peculiar type of wood, called reaction wood. In gymnosperm species,
29 reaction wood is formed on the lower side of the tilted axis (compression wood), while in
30 angiosperm species it is formed on the upper side (tension wood). Whatever the species
31 considered, the process of axis reorientation is always based on circumferential
32 heterogeneity in cambial region (cambial zone, differentiating and maturing zone)
33 activity occurring at 3 distinct structural levels:

34 - at the macroscopic level, the division and differentiation of the cambial initials is
35 controlled differently between the upper and the lower side of the trunk. This can lead to
36 an eccentric growth that causes the reaction wood side to be often wider than the opposite
37 side (Dadswell and Wardrop 1949; Almeras et al. 2005);

38 - at the mesoscopic level, proportions of the various cells types (fibres, vessels,
39 ray and axial parenchyma) constituting secondary xylem can vary substantially between
40 normal and reaction wood (Onaka 1949; Jourez et al. 2001; Ruelle et al. 2006);

41 - at the microscopic level, fibres produced during the reaction process strongly
42 differ structurally from normal fibres. This occurs through the modulation of various
43 structural features: (i) secondary wall fibre thickness, that tends to increase in some
44 species (Ruelle et al. 2006); (ii) size and orientation (MFA) of secondary wall cellulose
45 microfibrils: Washusen and Evans (2001) reported an increase of microfibrils size in
46 tension wood and MFA is known to be lower in tension wood and larger (up to 45°) in

47 compression wood (Timell 1986; Yoshida et al. 2000; Yoshizawa et al. 2000; Barnett
48 2004; Clair et al. 2006a); (iii) organization and chemical composition of
49 hemicellulose/lignin matrix surrounding cellulose microfibrils (Pilate et al. 2004;
50 Gorshkova and Morvan 2006).

51 The mechanism allowing reorientation of the axis originates in structural
52 modifications at the cell-wall level. Indeed, these micro-structural modifications induce
53 in wood a spontaneous tendency to strain during its maturation process (Boyd 1977;
54 Yamamoto 1998; Bamber 2001; Yamamoto et al. 2002). The maturation process of cell
55 wall can be subdivided in steps from cell expansion, secondary wall formation and
56 lignification to cell death (Plomion et al. 2001). During this process compression wood
57 tends to swell and tension wood tends to shrink. This tendency is impeded because
58 reaction wood is stuck to the core of old wood, resulting in a state of mechanical stress
59 (compression or tension), called maturation stress. The asymmetry of longitudinal
60 maturation stress around the circumference results in a bending moment generating a
61 change in curvature and thus a reorientation movement (Archer 1986). The efficiency of
62 this mechanism depends on the difference between the force acting on the reaction wood
63 side and the force acting on the opposite side. The magnitude of the force acting on one
64 side is the integral of the product of the area of maturing wood by the magnitude of the
65 maturation stress in wood. The magnitude of maturation stress in wood, in turn, can be
66 viewed as the product of the maturation strain by wood Young's modulus of wood.
67 Finally, Young's modulus can be expressed as the product of wood density by the
68 specific modulus of wood material elasticity (Almeras et al. 2005).

69 All four of these biomechanical factors, i.e. maturation stress asymmetry and
70 magnitude, Young's modulus of wood and specific modulus of wood material can be
71 controlled through modulations of cambial activity at the above-mentioned levels.

72 Eccentric growth controls the area of reaction wood and opposite wood. Proportions of
73 each cell type in the xylem partly control the specific modulus of elasticity of wood.
74 Fibre wall thickness controls wood density. Cellulose microfibril geometry and matrix
75 composition partly control specific modulus of elasticity and directly control sign and
76 magnitude of maturation strain (Okuyama et al. 1995; Yamamoto 1998). The mechanical
77 effect of these structural modifications can be predicted by mechanical models acting at
78 different levels. At the macroscopic level, reaction efficiency can be computed using
79 beam theory and the principles of its application to a growing structure (Fournier et al.
80 1994a). Fournier and coworkers model (1994a) takes into account the effects of eccentric
81 growth, modulus of elasticity and maturation strain (Almeras et al. 2005). At the
82 mesoscopic level, the effect of wood anatomy (i.e. the proportions and organisation of the
83 different cell types) can be predicted by homogenization procedures (Badel 1999). At the
84 microscopic level, cell wall micromechanical models allow to predict wood specific
85 modulus of elasticity and magnitude and sign of maturation strain (Yamamoto et al.
86 1998; Yamamoto et al. 2002). These models take as input data quantitative information
87 about cell wall organisation at the microscopic and ultra-structural levels, cell wall
88 chemical composition, and timing of cell wall differentiation and lignification.

89 The structure of reaction wood fibres generally differs from that of normal wood
90 fibres. In gymnosperms, compression wood fibres typically have a round shape,
91 intercellular spaces and cracks in the cell wall (Timell 1986). Their wall is thick and
92 heavily lignified, and the microfibrils are oriented at a wide angle with respect to the fibre
93 axis. Among angiosperms, diversity in the form of tension wood fibres has long been
94 recognized (Onaka 1949; Clair et al. 2006b). The most typical form of angiosperm
95 tension wood is characterized by the development of a so-called gelatinous layer (G-
96 layer). The G-layer is essentially made up of highly crystalline cellulose (Norberg and

97 Meier 1966; Côté et al. 1969), with a very low microfibril angle (Fujita et al. 1974).
98 However, several species do not develop G-fibres, while showing evidence of tension
99 wood production (Fisher and Stevenson 1981; Clair et al. 2006b).

100 During an exploration of biomechanical strategies of tropical rainforest species,
101 trees from *Laetia procera* species proved to be very efficient in restoring verticality after
102 accidental leaning (Almeras et al. 2005). Moreover, dissymmetry in the magnitude of
103 maturation strain was identified as the leading factor determining efficiency. The
104 maturation strain of tension wood was especially high in this species and tension wood
105 fibres presented a peculiar polylamellated structure. In order to check whether this
106 macroscopic behaviour was related to characteristic structural features, tension wood and
107 opposite wood were investigated using complementary techniques. In this way, optical
108 and electronic microscopy, histo-chemical reaction and UV microspectrophotometry
109 allowed us to obtain quantitative measurement about the structure and qualitative and
110 semi-quantitative information about the chemical composition of the secondary wall and
111 of the fibres.

112 MATERIAL AND METHODS

113 Plant material and sampling

114 *Laetia procera* (Poepp.) Eichler (Flacourtiaceae) is rare to locally frequent in primary and
115 secondary neo-tropical forests, on sandy soil.

116 Five trees were selected in the same area in French Guyana, near Kourou. Their
117 diameter at breast height (DBH) ranged between 19 and 28 cm (Table 1).

118 All trees were chosen because they were exhibiting a reorientation process after
119 some accidental inclination. This was verified *in situ* by mechanical estimation of growth
120 strain (GS). Experimentally, maturation strain can be estimated by releasing the

121 longitudinal stress at the surface of wood and measuring the resulting strain, referred to
122 as residual growth strain (GS). Growth strain is the sum of the maturation and support
123 strains. At the periphery of the trunk, where measurements were done, support strain are
124 due to the support of the newly formed layer and so are close to zero. Thus, growth strain
125 (GS) is very close to maturation strain. In the following text we will use GS, since it is
126 what has been experimentally measured.

127 GS were evaluated using the “single hole” method (Fournier et al. 1994b; Clair et
128 al. 2003; Almeras et al. 2005). This method gives the value of the displacement between
129 two pins, hammered onto the trunk (after local debarking) at a 45 mm distance from each
130 other. A 20mm-deep, 20mm-wide hole is drilled at the mid-point between the two pins. A
131 displacement is measured (in μm) and converted into a strain (in %) using a calibration
132 factor: 9.6×10^{-4} corresponding to a calibration made on *Eperua Falcata* (Fournier et al.
133 1994b), a tropical hardwood species with properties similar to those of *Laetia procera*.

134 Eight measurements (equally spaced around the circumference, i.e. every 45°)
135 were performed at breast height on each tree. The first measurement position was located
136 on the upper side of the leaning trunk. Two wood samples were taken, above and below
137 the holes resulting from the measurement method, for anatomical and structural studies.
138 Observations were made on both samples to ensure homogeneity of the studied wood
139 (Fig. 1).

140 Methods

141 First, classical optical microscopy on stained sections (including Wiesner reaction) was
142 used for all the 5 trees, in order to check if there were main differences between trees or
143 if the variation varied from one tree to another. Then, other techniques (Scanning
144 Electron Microscopy, UV microspectrophotometry) were only applied to the tree with the
145 highest contrast in GS between upper and lower part, Lp1 (Table 1).

146 Optical microscopy

147 Cross sections (thickness: 24 μm) were made with a sliding microtome using disposable
148 razor blades (Feather N35). Sections were stained with safranin/fast green according to
149 the protocol described by Yoshida et al. (2002). Safranin stains lignified tissues in red
150 and fast green stains both lignified and un-lignified tissues in green.

151 Wiesner reaction

152 Cross sections (thickness: 12 μm) were made on opposite and tension wood specimens.
153 Wiesner reaction was performed on these sections by pouring a few drops of 2 %
154 phloroglucinol ethanol solution on the section mounted on a glass-slide, adding one drop
155 of 35 % HCl and covering the section with a cover slip.

156 The Wiesner reactive reacts with coniferyl (G) and synapyl (S) aldehyde units in
157 lignin. The higher the Klason-lignin content the stronger the intensity of the red
158 coloration (Yoshizawa et al. 2000). This result provide us to do a comparison between
159 samples, i.e. a semi-quantitative analysis. As the coloration is not permanent, observation
160 was performed during the 20 minutes after the beginning of the reaction.

161 UV microspectrophotometry

162 After dehydration through a graded ethanol series, the sections were embedded in epoxy
163 resin. Thin cross sections (thickness: 1 μm) were cut with a diamond knife, mounted on
164 quartz microscope slides, overlaid with a drop of non-UV-absorbing glycerin, and
165 covered with a quartz cover slip (Okuyama et al. 1998). The sections were observed
166 under a microspectrophotometer (Zeiss MPM800). The scanning range of the wavelength
167 was 250-350nm, the step of the wavelength scanning was 1 nm, and the bandwidth was
168 adjusted to 5 nm. UV absorption spectra were obtained at various locations inside the
169 secondary wall of opposite and tension wood fibres using a beam spot of 0.5 μm

170 diameter. The absorption spectra directly provide information on cell wall lignin content
171 (Okuyama et al. 1998; Gindl 2002; Yoshida et al. 2002); the higher the absorption, the
172 more lignified the wall. Results from this technique can be used to make a comparison
173 between specimen; *ie* a semi-quantitative analysis among samples.

174 Each measurement for one position (one part of fibre wall) was repeated 8 times.
175 For each specimen the absorption spectrum of the secondary wall was taken at least on 5
176 different fibres and averaged to determine the UV absorption spectrum of the specimen.
177 The microspectrophotometer settings were: objective lens magnification: $\times 100$; program:
178 Lambdascan; (for more detailed information see Okuyama et al. 1998).

179 Field-Emission Scanning Electron Microscopy (FE-SEM)

180 Observations were made in both transverse and longitudinal planes. Sample geometries
181 were $7 \times 5 \times 1 \text{ mm}^3$ and $5 \times 1 \times 7 \text{ mm}^3$, respectively (R \times T \times L). Samples were dehydrated
182 through a graded ethanol series and then processed using the *t*-butanol freeze-drying
183 method. In order to observe cellulose microfibrils of lignified layers, a lignin extraction
184 treatment (NaCl 0.6%, CH₃COOH 0.13% in distilled water during 40 hours) was
185 performed on longitudinal sections. The dried samples were mounted on aluminium stubs
186 and lightly sputter-coated with platinum. Samples were observed by FE-SEM (Hitachi, S-
187 4500) at an accelerating voltage of 3 kV.

188 Microfibril angle (MFA) and diameter of cellulose aggregates were measured
189 from direct observations by SEM on samples from tree Lp1. These measurements were
190 made on 10 pictures per sample with magnifications from $\times 30k$ to $\times 70k$ and on about
191 20 microfibrils per picture for MFA and on 10 areas of about 5000 nm^2 for the diameter
192 of cellulose aggregates. Examples of images used for these measurements are shown in
193 Fig. 2.

194 Statistical analysis

195 Results from MFA and cellulose aggregates measurements were compared to highlight
196 significant differences between tension and opposite wood samples. We used the bilateral
197 Student test to account for the significance of these results.

198 **RESULTS**

199 Growth strain measurements

200 Measurements clearly show that wood located on the upper side exhibits much higher
201 tensile growth strains than wood located in all other position (Table 1). Measurements
202 performed on the lower (opposite) side do not present significant difference in
203 mechanical stressing with lateral position. Upper wood layer positions with very high
204 growth strains are called tension wood (TW) in the next paragraphs while other positions
205 are named opposite wood (OW) or lateral wood.

206 Considering data reported by Archer (1986) and more recent studies (Yoshida et
207 al. 2000; Yoshizawa et al. 2000; Clair et al. 2006b), GS observed in tension wood are in
208 the upper range of reported values.

209 Structure of the fibre wall

210 Poly laminate secondary wall of tension wood fibres

211 Optical microscopy observations after safranin/fast green staining show a homogeneous
212 typical secondary wall in opposite wood fibres, while a peculiar poly laminate secondary
213 wall structure is observed in tension wood fibres (Fig. 3). This structure consists of an
214 alternance of thick and thin layers. This peculiar secondary wall stains as a typical
215 gelatinous layer (G-layer), *i.e.* in green without any touch of red as in *Populus*
216 *euramericana* (Jourez et al. 2001) or *Eperua falcata* (Satiat-Jeunemaitre 1986).

217 Observation of transversal and longitudinal sections by Scanning Electron
218 Microscopy (SEM) confirms that the polylaminate structure of the secondary wall occurs
219 in tension wood but not in lateral or opposite wood fibres (Fig. 4 and 5). The number of
220 thin layers has been counted on tension wood specimens; results are given in Table 2.
221 There was an average of 5 to 6 thin layers with thick layers between them. Thick layers
222 are approximately ten times thicker than thin layers (Table 2).

223 Inner thin layer

224 Observations of longitudinal sections (Fig. 6a) also show a lignified layer inside the
225 lumen of tension wood fibres; this inner layer allowed us to prospect the nature and the
226 structure of thin layers observed in the polylaminate secondary wall. The aspect of this
227 layer before (Fig. 6b) and after (Fig. 6c) lignin extraction treatment highlights its lignified
228 feature and its large MFA. These features are typical of the S₃ layer commonly observed
229 in the cell wall of opposite wood fibres (Fig. 7a).

230 Organisation of cellulose in the secondary wall

231 MFA was very low (close to fibre axis) in the thick layers of tension wood fibres and
232 more than three fold larger (15 to 20°) in opposite wood (p<0.001) (Table 3).
233 Unfortunately we were unable to accurately measure MFA in intermediate thin layer.

234 Diameter of cellulose aggregates is in the range of values reported by Fahlen and
235 Salmen (2003) on *Picea abies*, *i.e.* between 18 and 23 nm, and is lower in opposite wood
236 (p<0.001) than in tension wood, respectively 18.4 and 21.9 nm.

237 Lignification features of tension wood fibres

238 Wiesner reaction

239 Intensity of the Wiesner reaction gives qualitative information on cell wall lignification
240 features. Polylaminate tension wood fibres appear less lignified than opposite wood fibres
241 (Fig. 8). In TW fibres the reaction is stronger in the outer part and becomes weaker
242 towards the centre. Some TW fibres have stronger reaction intensity than others; some of
243 them even show a lack of reaction on the polylaminate structure although the S₁ layer and
244 the primary wall are stained in red by the reaction (Fig. 9). This could mean that various
245 types of tension wood fibres can be observed.

246 Compared to typical G-layers, known to have very low lignin contents, the
247 secondary wall of *Laetia* TW presents lignin within the thick layers and the coloration
248 inside thin ones indicates a higher amount inside them.

249 UV microspectrophotometry

250 The average absorption spectra for the S₂ layer of a opposite wood sample (Lp1-5) and
251 for thick and thin layers of the secondary wall of a tension wood specimen (Lp1-2) are
252 given in Fig. 10.

253 In tension wood, the average absorption, and therefore polylaminate layer lignin
254 content, is lower than in the S₂ layer of opposite wood. Actually absorbance values in
255 tension wood specimen ranges from 0.15 to 0.24 at 280 nm and from 0.14 to 0.22 at 270
256 nm. In opposite wood absorbance values are higher than in tension wood and ranges from
257 0.34 to 0.53 at 280 nm and from 0.31 to 0.47 at 270 nm. Moreover the average absorption
258 of the whole fibre at 270 and 280 nm decreases with increasing growth strain values
259 (Table 4 and fig. 11).

260 UV microspectrophotometry also shows that lignification of TW is stronger in
261 secondary wall thin layers than in the thick layer. Thus, intermediate thin layers are
262 chemically different.

263 The absorption ratio A_{280}/A_{260} markedly depends on the ratio of syringylpropane
264 (S) to guaiacylpropane (G) units. Actually the decrease of this ratio corresponds to an
265 increasing S/G ratio (Okuyama et al. 1998; Yoshida et al. 2002). This ratio for tension
266 wood specimens is largely dominated by the properties of thick layers, because of the
267 prominent proportion of these layers compared to thin layers. According to our results,
268 S/G ratio increases with growth strains, with a good relationship (Table 4 and Fig. 12).
269 This evolution has been also described in some other species differentiating or not a G-
270 layer in their tension wood, such as eucalyptus (Baillères et al. 1995) or *Liriodendron*
271 *tulipifera* (Yoshida et al. 2002).

272 DISCUSSION

273 Observations made on *Laetia procera* tension wood show a polylaminate structure of the
274 secondary wall with the alternance of lightly lignified thick layers, with microfibrils
275 almost aligned to the cell main axis, and more lignified thin layers in which it was not
276 possible to measure microfibrils orientation. This kind of polylaminate structure has
277 previously been observed in bamboo cells (Parameswaran and Liese 1976). In a recent
278 study screening the anatomical diversity of tension wood among tropical dicotyledonous
279 species (Clair et al. 2006b), similar features were observed in tension wood of an other
280 Flacourtiaceae, *Casearia javitensis*. Moreover Daniel and Nilsson (1996) observed this
281 structure in a species from the Flacourtiaceae family, *Homalium foetidum*, but in their
282 study its occurrence was not identified as a tension wood feature. Observation of this

283 peculiar structure in tension wood fibres emphasises the idea exposed in Clair et al.
284 (2006b) on the difficulty to classify tension wood structures.

285 The very low MFA observed in thick layers is similar to what is usually observed
286 in tension wood fibres, with or without G-layer (Norberg and Meier 1966; Chaffey 2000;
287 Ruelle et al. 2006). The microfibrils of the inner thin layer of these cells appear less
288 organised and lie at a larger angle than those of thick layers. In their study on *Homalium*
289 *foetidum*, Daniel and Nilsson (1996) observed differences in microfibril angle between
290 thick and thin layers. These various observations lead us to hypothesise that cellulose
291 organisation in the thin layers is (i) different from the one of thick layers and (ii) similar
292 to the one observed in the inner thin layer, so that all these thin layers look like
293 successive S₃ layers between thick layers.

294 Prodhan et al. (1995) shows that G-layer in *Fraxinus mandshurica* is lignified, in
295 the same way as in *Laetia procera*, with a higher content of lignin in the outer part of the
296 G-layer. Similar observations were made by Gierlinger and Schwanninger (2006), i.e. a
297 higher lignification in the outer part of G layer, but in their work they found a very weak
298 content of lignin in the rest of the G layer. These observations support the statement
299 (Terashima 1990) that there is a lignification gradient from outer to inner part of the cell
300 wall during fibre development. However the alternance of more lignified layers raises
301 several questions about the development of the secondary wall and about its role in the
302 very efficient strategy of reorientation observed in this species. In current fibre mechanics
303 models, maturation strain associated to the end of the lignification process is assumed to
304 occur simultaneously in the whole S₂ or G-layer. Moreover, it is known that the final pre-
305 stressing values in a multilayered composite depend on the history of layer deposition
306 (Yamamoto et al. 2002). This effect of successive step construction in a material on field
307 of stresses is also true for various natural or man-made structures such as trees, bridges,

308 etc. (Guitard et al. 1999; Malzbender 2004). It may be important to know whether each
309 thick layer and associated thin layer is fully lignified successively or if the lignification
310 process occurs after the deposition of all the layers.

311 This raises questions about the rhythm of secondary wall development. Hosoo et al.
312 (2002; 2003) showed diurnal periodicity in the deposition of cell wall components on the
313 innermost surface of developing cells. This seems to indicate that there is diurnal
314 periodicity in cell wall formation, corresponding to the 24-h light-dark cycle. Question
315 about relation between thick and thin layers alternance and circadian rhythm should be
316 investigated, and young trees artificially inclined in controlled conditions can be a good
317 material for such study, knowing that tension wood will be rapidly induced on upper part
318 of the young tree (Jourez et al. 2001).

319 The multilayered tension wood has been, until now, only found in others genus of
320 the Flacourtiaceae Family (Daniel and Nilsson 1996; Clair et al. 2006b). It should be
321 interesting to investigate whether this feature occurs in the whole family.

322

ACKNOWLEDGMENTS

Many thanks to Tancrede Almeras for his critical review of this paper and Ivan Scotti for English corrections.

REFERENCES

- Almeras T, Thibaut A, Gril J (2005) Effect of circumferential heterogeneity of wood maturation strain, modulus of elasticity and radial growth on the regulation of stem orientation in trees. *Trees* 19:457-467
- Archer RR (1986) *Growth stresses and strains in trees*. Springer-Verlag, Berlin Heidelberg New-York

- Badel E (1999) Détermination des propriétés élastiques et du retrait d'un cerne annuel de chêne dans le plan transverse : description de la morphologie, mesures des propriétés microscopiques et calculs d'homogénéisation
- Baillères H, Chanson B, Fournier M, Tollier MT, Monties B (1995) Structure, composition chimique et retraits de maturation du bois chez les clones d'eucalyptus. *Ann Sci For* 52:157-172
- Bamber R (2001) A general theory for the origin of growth stresses in reaction wood : how trees stay upright. *IAWA J* 22:205-212
- Barnett JR (2004) Cellulose microfibril angle in the cell wall of wood fibres. *Biol Rev* 79:461-472
- Boyd JD (1977) Basic cause of differentiation of tension wood and compression wood. *Aust For Res* 7:121-143
- Chaffey N (2000) Microfibril orientation in wood cells : new angles on an old topic. *Trends Plant Sci* 5:360-362
- Clair B, Almeras T, Sugiyama J (2006a) Compression stress in opposite wood of angiosperms: observations in chestnut, mani and poplar. *Ann. For. Sci.* 63:507-510
- Clair B, Ruelle J, Beauchêne J, Prevost MF, Fournier M (2006b) Tension wood and opposite wood in 21 tropical rainforest species. 1. About the presence of G layer. *IAWA J* 27:329-338
- Clair B, Ruelle J, Thibaut B (2003) Relationship between growth stresses, mechano-physical properties and proportion of fibre with gelatinous layer in chestnut (*Castanea Sativa* Mill.). *Holzforchung* 57:189-195
- Côté WAJ, Day AC, Timell TE (1969) A contribution to the ultrastructure of tension wood fibers. *Wood Sci Technol* 3:257-271
- Dadswell HE, Wardrop AB (1949) What is reaction wood? *Australian Forestry* 13:22-33
- Daniel G, Nilsson T (1996) Poly laminate concentric cell wall layering in fibres of *Homalium foetidum* and its effect on degradation by microfungi. *Recent Advances in WOOD ANATOMY*, New Zealand Forest Research Institute:369-372
- Fahlen J, Salmen L (2003) Cross-sectional structure of the secondary wall of wood fibers as affected by processing. *J Mater Sci* 38:119-126
- Fisher JB, Stevenson JW (1981) Occurrence of reaction wood in branches of Dicotyledons and its role in tree architecture. *Bot Gaz* 142:82-95
- Fournier M, Baillères H, Chanson B (1994a) Tree biomechanics: growth, cumulative prestress, and reorientations. *Biomimetics* 2:229-251
- Fournier M, Chanson B, Thibaut B, Guitard D (1994b) Mesure des déformations résiduelles de croissance à la surface des arbres, en relation avec leur morphologie. Observation sur différentes espèces. *Ann Sci for* 51:249-266

- Fujita M, Saiki H , Harada H (1974) Electron Microscopy of Microtubules and Cellulose Microfibrils in Secondary Wall Formation of Poplar Tension Wood Fibers. *Mokuzai Gakkaishi* 20:147-156
- Gierlinger N , Schwanninger M (2006) Chemical Imaging of Poplar Wood Cell Walls by Confocal Raman Microscopy. *Plant Physiol* 140:1246-1254
- Gindl W (2002) Comparing Mechanical properties of normal and compression wood in Norway Spruce: the role of lignin in compression parallel to the grain. *Holzforschung* 56:395-401
- Gorshkova T , Morvan C (2006) Secondary cell-wall assembly in flax phloem fibres: role of galactans. *Planta* 223:149-158
- Guitard D, Masse M, Yamamoto H , Okuyama T (1999) Growth stress generation: a new mechanical model of the dimensional change of wood cells during maturation. *J Wood Sci* 45:384-391
- Hosoo Y, Yoshida M, Imai T , Okuyama T (2002) Diurnal difference in the amount of immunogold-labeled glucomannans detected with field emission scanning electron microscopy at the innermost surface of developing secondary walls of differentiating conifer tracheids. *Planta* 215:1006-1012
- Hosoo Y, Yoshida M, Imai T , Okuyama T (2003) Diurnal Differences in the Innermost Surface of the S2 Layer in Differentiating Tracheids of *Cryptomeria japonica* Corresponding to a Light-Dark Cycle. *Holzforschung* 57:567-573
- Jourez B, Riboux A , Leclercq A (2001) Anatomical characteristics of tension wood and opposite wood in young inclined stems of poplar (*Populus euramericana* cv "Ghoy"). *IWA J* 22:133-157
- Malzbender J (2004) Mechanical and thermal stresses in multilayered materials. *J Appl Phys* 95:1780-1782
- Norberg PH , Meier H (1966) Physical and chemical properties of the gelatinous layer in tension wood fibres of Aspen (*Populus tremula* L.). *Holzforschung* 20:174-178
- Okuyama T, Takeda H, Yamamoto H , Yoshida M (1998) Relation between growth stress and lignin concentration in the cell wall: Ultraviolet microscopic spectral analysis. *J Wood Sci* 44
- Okuyama T, Yoshida M , Yamamoto H (1995) An estimation of the turgor pressure change as one of the factors of growth stress generation in cell walls. *Mokuzai Gakkaishi* 41:1070-1078
- Onaka F (1949) Studies on compression and tension wood. *Wood research, Bulletin of the Wood research Institute, Kyoto University, Japan* 24:1-88
- Parameswaran N , Liese W (1976) On the Fine Structure of Bamboo Fibres. *Wood Sci Technol* 10:231-246

- Pilate G, Chabbert B, Cathala B, Yoshinaga A, Leple JC, Laurans F, Lapierre C , Ruel K (2004) Lignification and tension wood. C R Biologies 327:889-901
- Plomion C, Leprovost G , Stokes A (2001) Wood formation in Trees. Plant Physiol 127:1513-1523
- Prodhan AKMA, Ohtani J, Funada R, Abe H , Fukazawa K (1995) Ultrastructure investigation of tension wood fibre in *Fraxinus mandshurica* Rupr. var. *japonica* Maxim. Ann Botany 75:311-317
- Ruelle J, Clair B, Beauchêne J, Prevost MF , Fournier M (2006) Tension wood and opposite wood in 21 tropical rainforest species. 2. Comparison of some anatomical criteria. IAWA J 27:341-376
- Satiat-Jeunemaitre B (1986) Cell wall morphogenesis and structure in tropical tension wood. IAWA Bull. 7:155-164
- Sinnott EW (1952) Reaction Wood and the Regulation of Tree Form. Am J Bot 39:69-78
- Terashima N (1990) A new mechanism for formation of a structurally ordered protolignin macromolecule in the cell wall of tree xylem. J Pulp Paper Sci 16:150-155
- Timell TE (1986) Compression wood in gymnosperms. Springer-Verlag, Berlin Heidelberg
- Washusen R , Evans R (2001) The association between cellulose crystallite width and tension wood occurrence in *Eucalyptus globulus*. IAWA Journal 22:235-243
- Yamamoto H (1998) Generation mechanism of growth stresses in wood cell walls : roles of lignin deposition and cellulose microfibril during cell wall maturation. Wood Sci Technol 22
- Yamamoto H, Kojima Y, Okuyama T, Abasolo WP , Gril J (2002) Origin of the Biomechanical properties of wood related to the fine structure of the multi-layered cell wall. J Biomech Eng 124:432-440
- Yamamoto H, Okuyama T , Yoshida M (1998) Growth stress generation and microfibril angle in reaction wood. Microfibril Angle in Wood. The proceedings of the IAWA / IUFRO international workshop on the *Significance of microfibril angle to wood quality*:225-239
- Yoshida M, Ohta H, Yamamoto H , Okuyama T (2002) Tensile growth stress and lignin distribution in the cell walls of yellow poplar, *Liriodendron tulipifera* Linn. Trees 16:457-464
- Yoshida M, Okuda T , Okuyama T (2000) Tension wood and growth stress induced by artificial inclination in *Liriodendron tulipifera* Linn. and *Prunus spachiana* Kitamura f. *ascendens* Kitamura. Ann. For. Sci. 57:739-746
- Yoshizawa N, Inami A, Miyake S, Ishiguri F , Yokota S (2000) Anatomy and lignin distribution of reaction wood in two *Magnolia* species. Wood Sci Technol 34:183-196
-

FIGURES LEGENDS

Fig. 1 Localization of specimen used for the experiments

Fig. 2 Example of images used for the measurements of microfibril angle on tension wood (a), opposite wood (b) and cellulose aggregates diameter on tension wood (c), opposite wood (d). Scale bars: 500 nm

Fig. 3 Cross sections of tension wood (a) and opposite wood (b) from *Laetia procera* stained with safranin/fast green. Scale bars: 25 μm

Fig. 4 Cross section of tension wood (a) and opposite wood (b) of *Laetia procera*, observed with SEM. Scale bars: 5 μm

Fig. 5 SEM observation of the polylaminate structure of the secondary wall in tension wood fibre on a longitudinal section of *Laetia procera*. Scale bar: 15 μm

Fig. 6 Longitudinal section of *Laetia procera* tension wood. (a) Observation of the lignified layer inside the lumen (scale bar: 15 μm). (b) Detail of the image a (scale bar: 1 μm). (c) Detail of the inner layer view from the lumen after a lignin extraction treatment (scale bar: 1 μm). Microfibril angle in the inner layer is very large.

Fig. 7 Longitudinal section of *Laetia procera* opposite wood. (a) Observation of the lignified layer inside the lumen (scale bar: 5 μm). (b) Detail of the image a (scale bar: 1 μm). (c) Detail of the inner layer view from the lumen after a lignin extraction treatment (scale bar: 1 μm). Microfibril angle in the inner layer is very large.

Fig. 8 Result of the Wiesner reaction on transversal sections of tension (a) and opposite (b) specimen of *Laetia Procera*. Scale bars: 20µm

Fig. 9 Detail of a transversal section of tension wood specimen, showing tension wood fibres with lack of Wiesner reaction. Scale bar: 10 µm

Fig. 10 UV absorption spectra of a tension wood (a) specimen (Lp1-2) and an opposite wood (b) specimen (Lp1-5) of Lp1 tree. Bars are standard deviations

Fig. 11 Absorbance at 280 nm (a) and 270 nm (b) versus growth strain values for specimen from Lp1 tree

Fig. 12 Absorbance ratio A280/A260 versus growth strain values of specimen from the tree Lp1

TABLES

Table 1 Diameter at breast height (DBH, in cm), Growth Strain (microstrains) means value, standard deviation and number of positions used for upper and lower side for each tree

Trees	DBH (cm)	Tension wood (TW)		Opposite wood (NW)		Upper - lower side means
		Mean of the upper side	Number of positions	Mean of the lower side	Number of positions	
Lp1	19	2714 ± 700	3	666 ± 293	3	2246
Lp2	23	2035 ± 625	2	515 ± 23	3	1520
Lp3	28	2701 ± 318	3	666 ± 247	3	2035
Lp4	22	1590 ± 681	3	582 ± 105	3	1008
Lp5	26	2912 ± 404	3	416 ± 200	3	2496

Table 2 Values and standard deviation of the various measurements on fibre secondary wall of tension wood specimen from Lp1 tree

Tree	specimen	GS (μ strain)	Thick layer thickness (μ m)	Thin layer			Thin layer thickness / thick layer thickness	
				Thickness (μ m)	number			
					min	mean		max
Lp1	1	3504	1.38 ± 0.26	0.08 ± 0.03	4	5.30	8	0.06
	2	2170	1.31 ± 0.15	0.13 ± 0.03	5	6.00	7	0.10
	3	2467	1.44 ± 0.52	0.15 ± 0.03	4	5.13	7	0.11

Table 3 MFA and diameter of cellulose aggregates (mean \pm SD) for each sample from Lp1 tree. TW: tension wood, OW: opposite wood, LW: lateral wood

Tree	Type of wood	Specimen	GS (μ strains)	Average MFA ($^{\circ}$) / specimen	Average MFA ($^{\circ}$) / type of wood	Average diameter of cellulose aggregates (nm) / specimen	Average diameter of cellulose aggregates (nm) / type of wood
Lp1	TW	1	3504	3.1 \pm 1.9	5.2 \pm 3.1	22.8 \pm 3.0	21.9 \pm 0.8
		2	2170	8.6 \pm 5.7		21.7 \pm 2.2	
		3	2467	3.8 \pm 2.3		21.3 \pm 3.3	
	LW	4	-115	16.6 \pm 4.8		18.3 \pm 1.6	
	OW	5	346	20.7 \pm 5.3		20.4 \pm 2.2	
	OW	6	922	16.2 \pm 6.2	17.5 \pm 2.8	17.2 \pm 1.9	18.4 \pm 1.6
	OW	7	730	13.9 \pm 4.8		16.4 \pm 2.1	
	LW	8	461	19.9 \pm 5.2		19.6 \pm 1.6	

Table 4 Absorbance at wavelengths 270 and 280 nm and ratio of absorbance A280/A260 of the various layers of specimen of *Laetia procera* n°1

Tree specimen			GS (μ strains)	Thick layers			Thin layers		
				A280	A270	A280/A260	A280	A270	A280/A260
Tension wood specimen	Lp1	1	3504	0.15	0.14	1.15	0.18	0.18	1.08
		2	2170	0.15	0.14	1.19	0.29	0.27	1.17
		3	2467	0.24	0.22	1.20	0.38	0.36	1.13
				S ₂ layers					
				A280	A270	A280/A260			
Opposite and lateral wood specimen		4	-115	0.45	0.40	1.27			
		5	346	0.44	0.40	1.31			
		6	922	0.37	0.33	1.25			
		7	730	0.34	0.31	1.25			
		8	461	0.53	0.47	1.30			

FIGURES

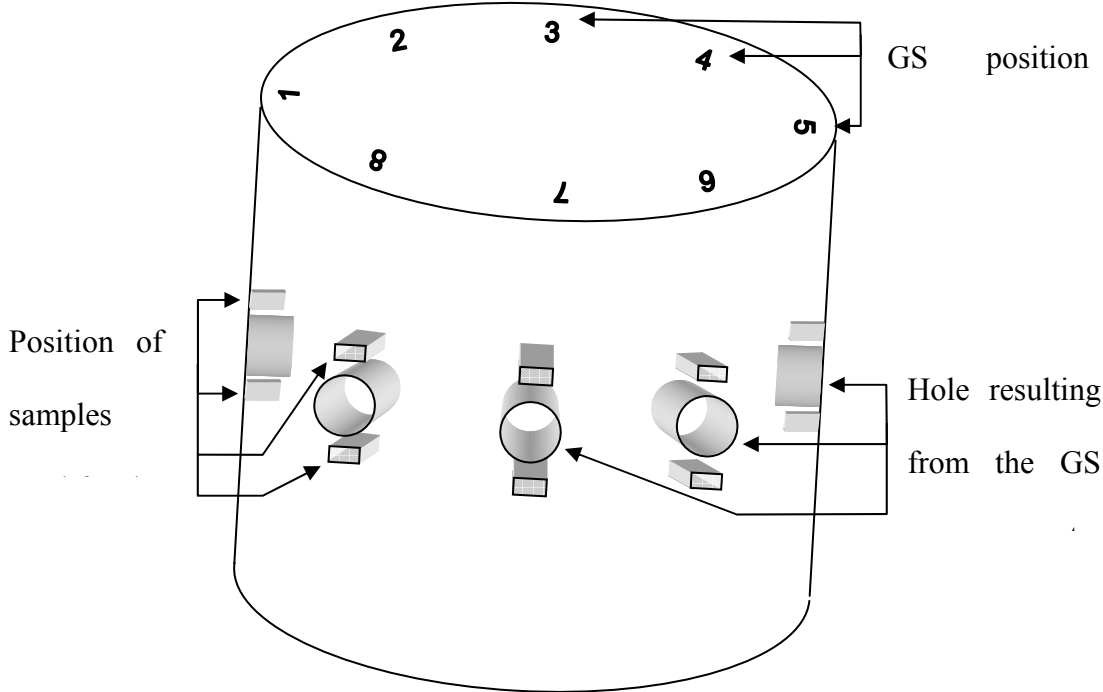


Fig. 1

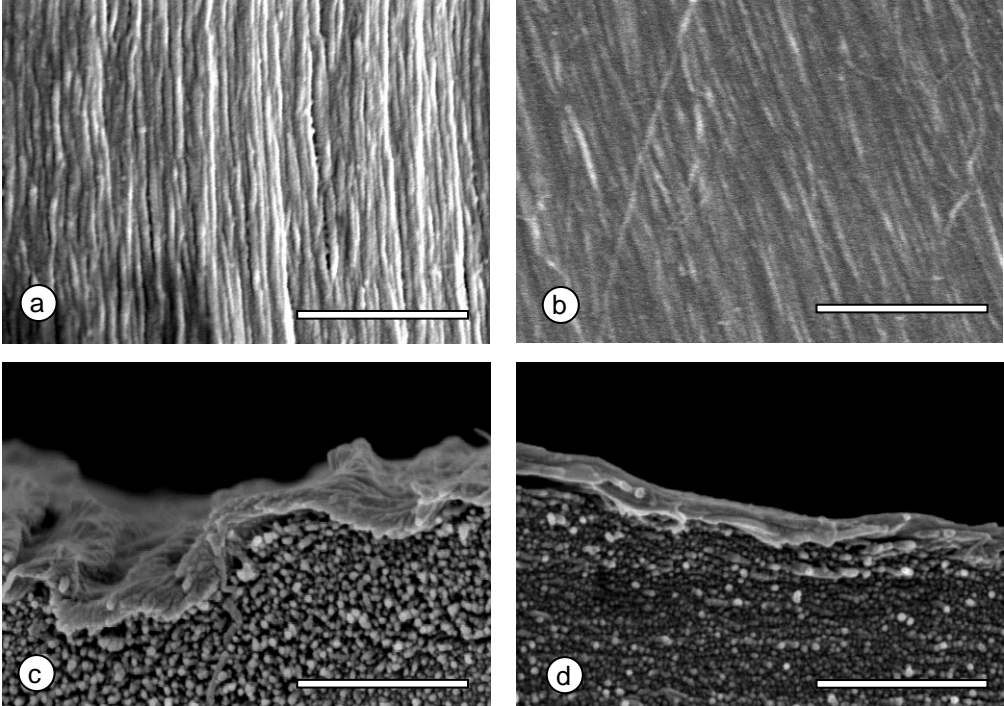


Fig. 2

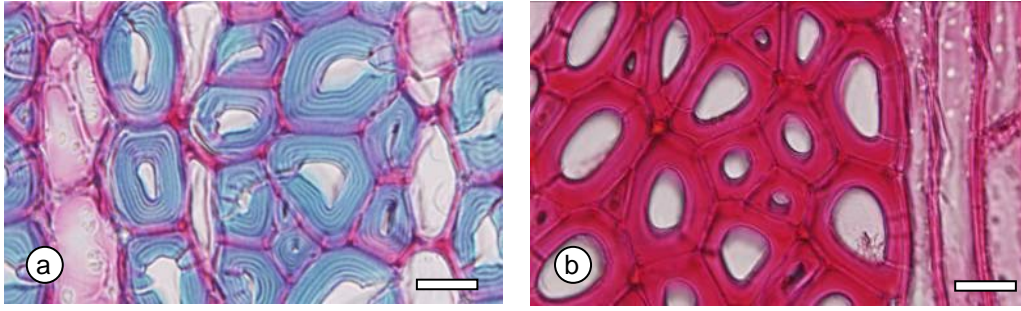


Fig. 3

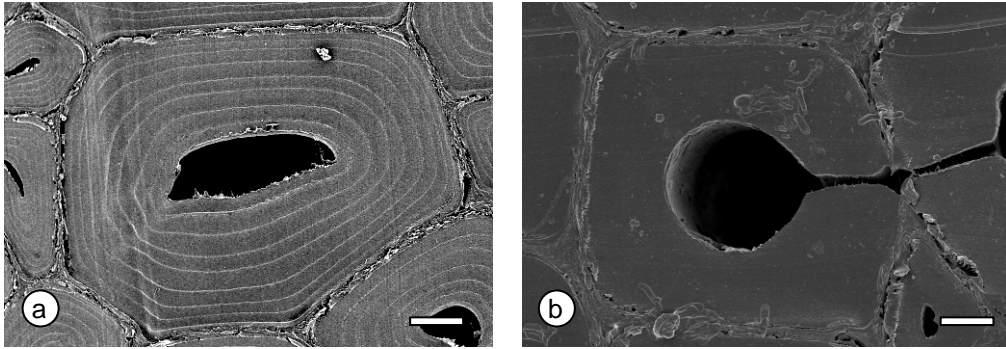


Fig. 4

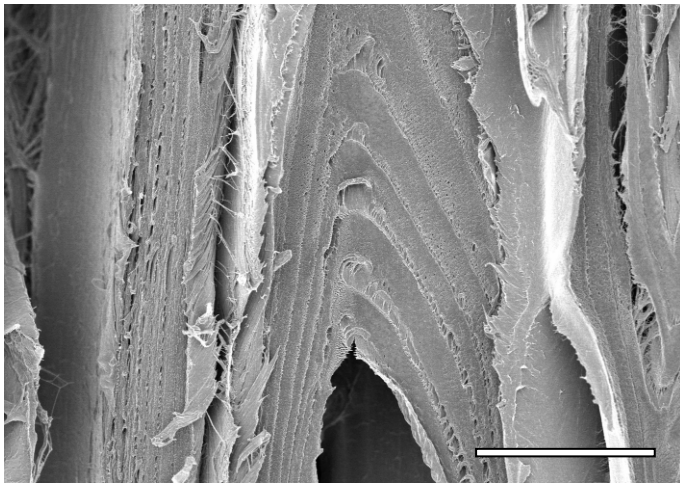


Fig. 5

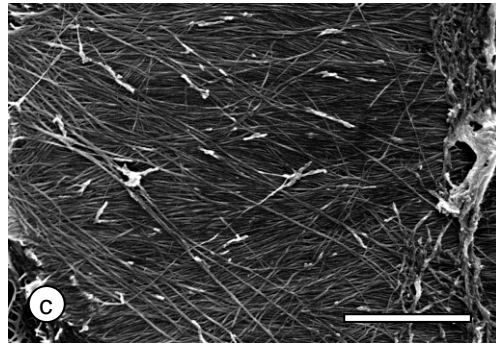
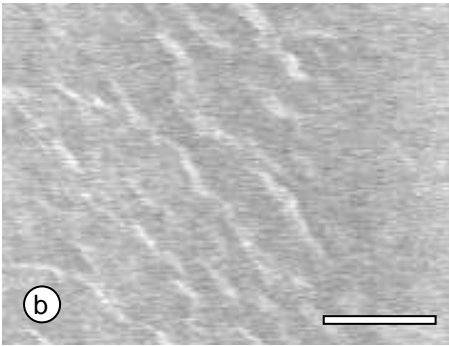
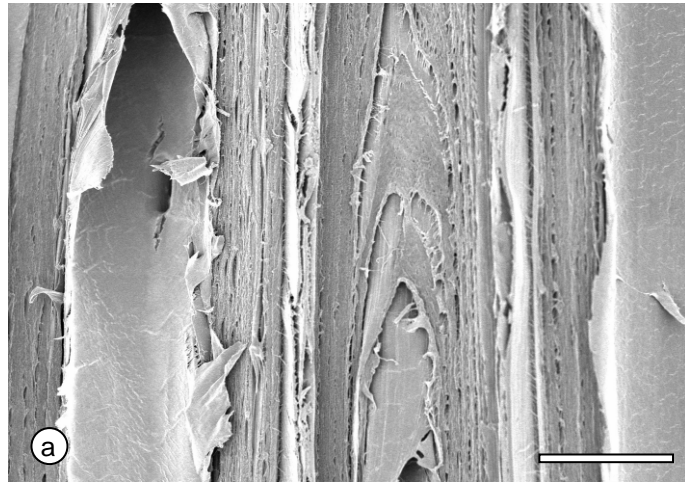


Fig. 6

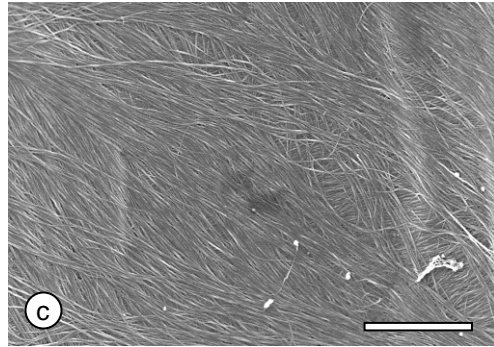
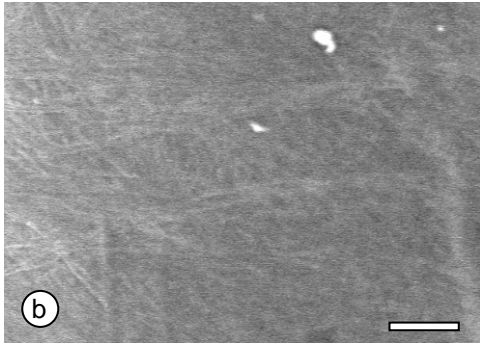
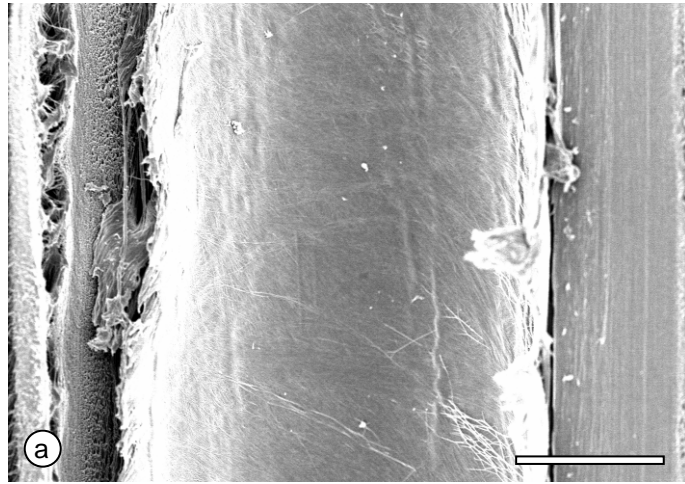


Fig. 7

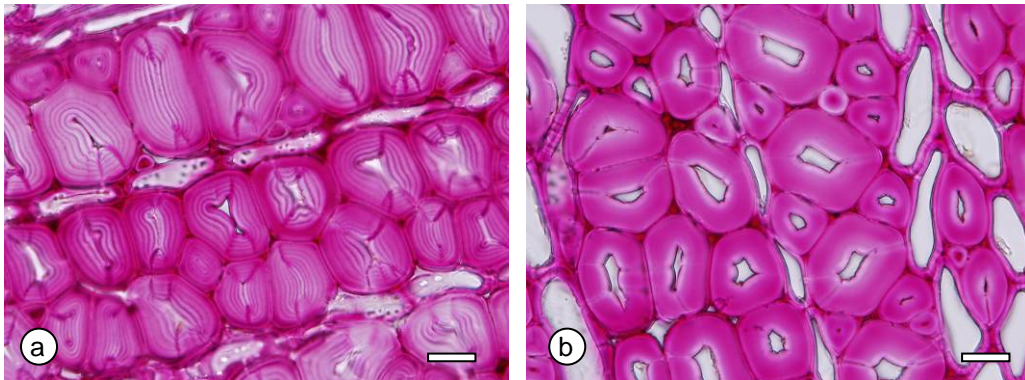


Fig. 8



Fig. 9

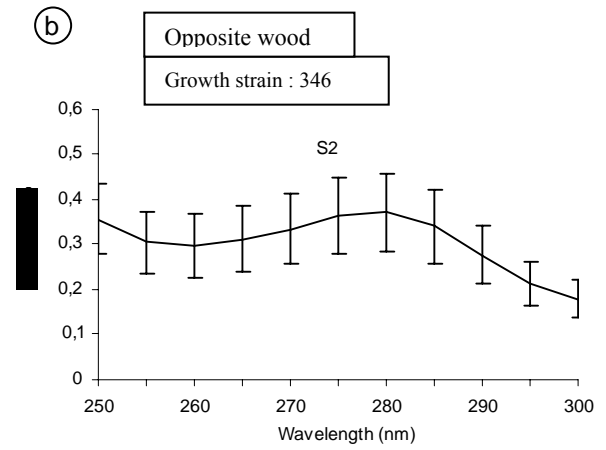
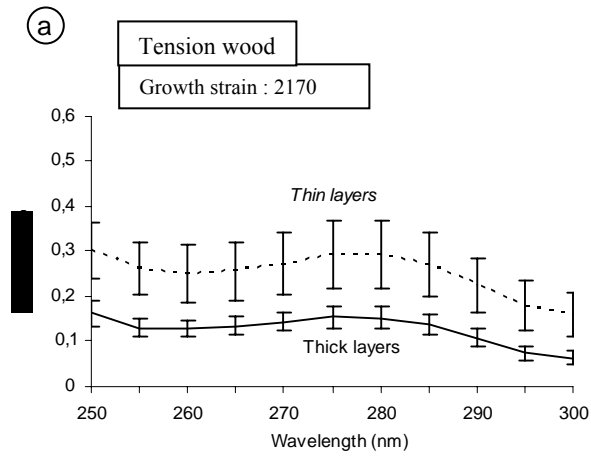


Fig. 10

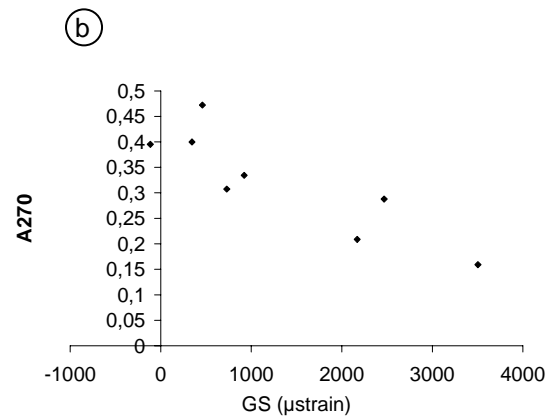
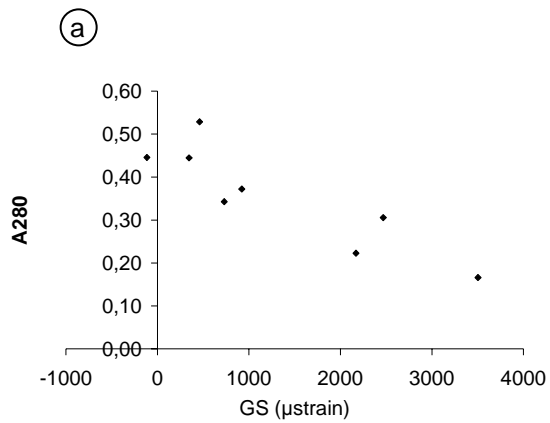


Fig. 11

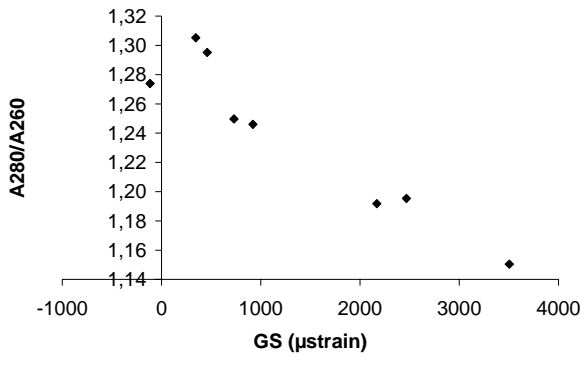


Fig. 12